

# Open-circuit voltage increase dynamics in high and low deposition rate polymorphous silicon solar cells

E. V. Johnson<sup>\*1</sup>, F. Dadouche<sup>2</sup>, M. E. Gueunier-Farret<sup>2</sup>, J. P. Kleider<sup>2</sup>, and P. Roca i Cabarrocas<sup>1</sup>

<sup>1</sup>LPICM, CNRS, École Polytechnique, 91128 Palaiseau, France

<sup>2</sup>LGEP, CNRS, Supélec, 11 rue Joliot-Curie, Plateau de Moulon, 91192 Gif-sur-Yvette, France

Received 30 July 2009, revised 2 November 2009, accepted 9 November 2009

Published online 19 January 2010

PACS 73.50.Pz, 84.60.Bk, 84.60.Jt

\* Corresponding author: e-mail erik.johnson@polytechnique.edu, Phone: +33 169 33 43 21, Fax: +33 169 33 43 33

The dynamics of the open-circuit voltage ( $V_{OC}$ ) of polymorphous silicon (pm-Si:H) solar cells deposited at high and low rates (8 and 1.5 Å/s, HR and LR) and containing lightly or heavily doped p-layers (LD or HD) are compared through *in situ*, variable intensity measurements during light-soaking (LS). The  $V_{OC}$ 's of the LR cells show an increase with LS, regardless of doping level, whereas the HR cells show decreasing  $V_{OC}$ 's. This result is in contrast to the changes predicted by the dark diode characteristics, which predict

increasing  $V_{OC}$  for all the devices. The device measurements are compared to the analogous measurements on co-deposited coplanar p-i layer stacks to determine whether the  $V_{OC}$  dynamics can be linked to changes in the p-layer doping efficiency during LS. The changes to the macroscopic electrical behaviour of the cell under varying light conditions are modelled using a simple, three parameter function, and are compared to results from a detailed, numerical modelling tool, AFORS-HET.

© 2010 WILEY-VCH Verlag GmbH & Co. KGaA, Weinheim

**1 Introduction** The relative stability under light-soaking of the efficiency of thin-film PIN photovoltaic cells fabricated using an intrinsic layer of polymorphous silicon (pm-Si:H) is partly due to the manner in which the macroscopic cell electrical parameters change with light-soaking (LS). In particular, the ever-present decrease in fill factor (FF) of these cells is often accompanied by an offsetting increase in open circuit voltage ( $V_{OC}$ ). However, this advantageous increase is not ubiquitous to all pm-Si:H cells, and has not been observed in pm-Si:H modules deposited at high rates (8 Å/s) although it has been observed for modules deposited at slightly lower rates (5 Å/s) [1]. Such an increase in  $V_{OC}$  has been previously noted by a number of authors for a-Si:H cells grown with hydrogen-dilution. The effect has been variously attributed to dopant activation in the p-layer [2], changes to the macroscopic properties of the i-layer [3], or finally, a specific redistribution of the recombination within the i-layer [4] that is evident from dark current-density–voltage ( $J$ – $V$ ) measurements. More recently, Yue et al. [5] studied the effect in NIP cells near the amorphous-nanocrystalline transition, and attributed it to the breakdown of a small nanocrystalline phase in the i-layer.

We explore the physical reasons behind the  $V_{OC}$  dynamics in pm-Si:H PIN's through *in situ* variable intensity method (VIM) measurements on PIN's during LS, through LS-dependent lateral dark-conductivity measurements on p-i layer stacks, and through both parametric and numerical modelling of the devices. We use these techniques to compare the dynamics of cells and stacks deposited at low rates (1.5 Å/s) to those at high rates (8 Å/s) and on identical cells with different p-layers.

**2 Experimental description** The samples for this study were deposited by radio-frequency plasma-enhanced chemical vapour deposition (rf-PECVD) in the ARCAM reactor, a multi-plasma, monochamber system [6].

**2.1 PIN and p-layer stack preparation** The PIN cells utilized for this study consisted of two sets of two cells. Each set contains a sample using a lightly doped (LD) p-a-SiC:H layer deposited with a TMB flow rate of 10 sccm, and one with a more heavily doped (HD) p-a-SiC:H layer (TMB = 20 sccm). The p-layers were ~150 Å thick. The first set of samples consists of two cells with the pm-Si:H intrinsic

layer deposited at low rate (LR, 1.5 Å/s), and the second set with layers deposited at higher rate (HR, 8 Å/s), but with all i-layers being 2500–2700 Å thick. For ease of nomenclature, the logical descriptive acronyms are used (e.g. HDHR for Heavily Doped, High Rate cell). The HR recipe has been recently used to produce high efficiency 10 cm × 10 cm modules [1], although the cells described herein are less efficient. The cells were finished using a 180 Å n-a-Si:H layer and were defined by a 0.126 cm<sup>2</sup> aluminium back contact. The cells were not annealed after deposition.

The PIN stack was co-deposited on both ASAHI Type-U SnO<sub>2</sub>, as well as Corning “Eagle” glass for use in the study of p-layer behaviour during light soaking (Section 3.2). The n-layers of the samples on glass were etched away and coplanar aluminium contacts were evaporated on top of the remaining i-layer.

**2.2 Light soaking** Light soaking of the samples was performed at 25 °C, under open circuit conditions, and over periods of up to 1000 min, with measurements taken at chosen intervals. A 150 W Xenon lamp was used with focussing optics and a neutral density filter to adjust the light intensity on the sample to ~100 mW/cm<sup>2</sup>. For the PIN’s, an automated variable illumination method (VIM) routine was invoked at various points during the light-soaking [7] using an automated neutral density filter wheel and the same Xenon light source to generate conditions from dark up to four suns illumination. The same set-up was used to perform the co-planar dark conductivity measurements on the p-layer stacks during light-soaking.

### 3 Results and discussion

**3.1 PIN light soaking studies** For the PIN cells, the most interesting parameter to be monitored during LS is  $V_{OC}$ . Figure 1 displays the dynamics of  $V_{OC}$  during the first 1000 min of LS for the four cells under study. The cells display the  $V_{OC}$  dynamics that have been noted in a previous

publication [1] – namely that for the LR cells, an increase is observed, whereas for the HR cells, a rapid decrease is observed. Another important element to note in Fig. 1 is that the more heavily doped p-layers result in a lower initial  $V_{OC}$  in both cases (although for the low-rate cells, the LS value is the same) suggesting that the LD p-layers are not in fact under-doped. The  $V_{OC}$  is therefore limited by factors other than an under-doped p-layer. This also strongly suggests that the dopant activation effect invoked in Ref. [2] is not the dominating effect in this case, as the opposite trend would be expected during LS.

In this paper, we aim to pin-point the source of increase/decrease on changes in the various layers. Already, the use of the VIM technique permits the observation of changes in the dark-diode characteristics,  $J_0$  and  $n$ . Interestingly, the changes in these parameters (using the classical formula ignoring photocarrier recombination,  $V_{OC} = nkT \ln(J_{SC}/J_0 - 1)$ ) predict an increase in  $V_{OC}$  for *all* the devices – the increasing value of  $n$  always overwhelming the increasing value of  $J_0$  – underlining the importance of the light-dependent study.

**3.2 p-i layer stack studies** As changes in the p-layer during light-soaking have been invoked as the source of the  $V_{OC}$  increase [2], studies on the p-i layer stacks have been performed in parallel with those of the PIN cells. An initial examination of the temperature dependent dark conductivity of the samples was performed, and is summarized in Table 1 for the as deposited state and after an anneal at 125 °C for 1 h.

The activation energies ( $E_A$ ) of Table 1 show that for the p-i stack structures used, it is the properties of the p-layer that are most strongly sampled, with the possible exception of the LDLR sample. Ignoring the LDLR sample, one may also note that in the annealed state, the relative differences in  $E_A$  correspond to the differences in LS  $V_{OC}$  (Fig. 1).

A parallel set of un-annealed p-i stacks were submitted to a room temperature conductivity test during LS over 1000 min, the results of which are presented in Fig. 2. A result for an annealed HDLR sample is also presented.

The results of Fig. 2 show that the conductivity of the p-layer increases dramatically in the HDLR sample (with a delay for the annealed sample), and more slightly for the LDLR sample (which as noted from Table 1, is not simply a reflection of changes in the p-layer). For all samples, a long-term decrease in conductivity is observed.

**3.3 Parametric modelling** To model the changes in the electrical parameters and link them to changes in the

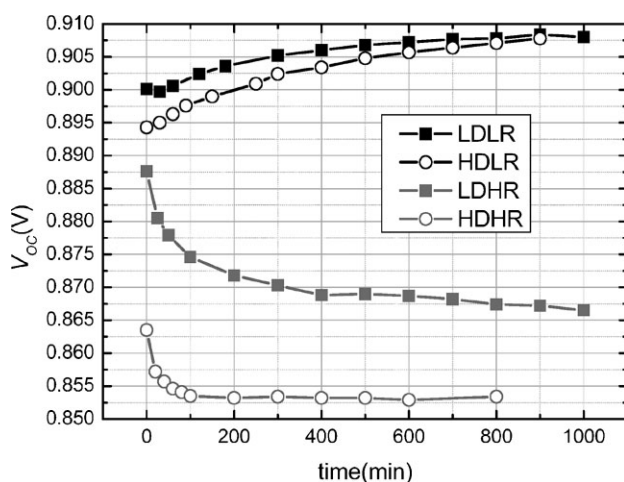


**Figure 1** Evolution of  $V_{OC}$  during LS for cells deposited at low and high deposition rates (LR and HR, respectively) and with lightly and heavily doped p-layers (LD and HD, respectively).

**Table 1** Measured activation energies for p-i layer stacks with coplanar aluminium contacts, before and after anneal.

	$E_A$ , as deposited (eV)	$E_A$ , annealed (eV)
LDLR	0.48	0.44
HDLR	0.29	0.29
LDHR	0.36	0.33
HDHR	0.34	0.34

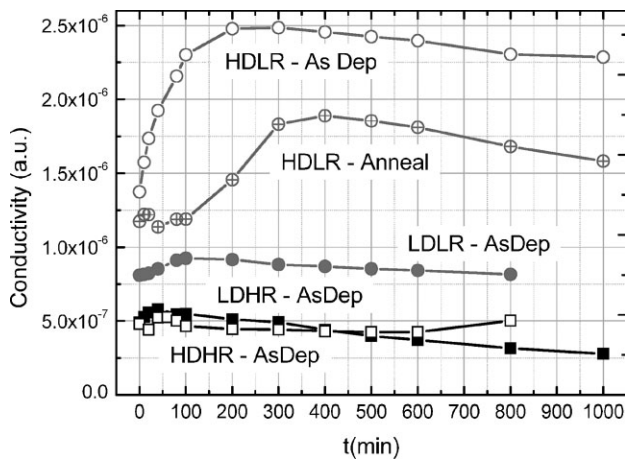


**Figure 2** Variations in conductivity during light-soaking of p-i layer stacks. “As Deposited” measurements are shown for all the samples, and a sample annealed at 125 °C for 30 min is also shown for the HDLR stack.

p-layer, a model for the voltage-dependent carrier collection in PIN structures is invoked, as first proposed by Crandall [8] and further developed by Repmann et al. [9] for tandem cells. In this model, the decrease in photocurrent due to recombination is modelled by a bias-voltage dependent function, as  $J_{ph} = J_{ph,0}\chi(V)$ , where

$$\chi(V) = \left( \frac{V - V_{bi}}{V_{\mu}} \right) \left( 1 - e^{V_{\mu}/(V - V_{bi})} \right), \quad (1)$$

in which  $V_{\mu} = d_i^2 / \mu \tau_{eff}$ ,  $d_i$  is the i-layer thickness,  $\mu \tau_{eff}$  is an effective mobility lifetime product for both holes and electrons, and  $V_{bi}$  is the built-in potential across the i-layer. Note that both modelling parameters  $V_{bi}$  and  $V_{\mu}$  are independent of light intensity. This model for the cell assumes that the recombination current is linear with carrier density – that is, that there is little redistribution of the field due to photo-generated and trapped carriers.

The theoretical independence on light intensity was tested for the cells of this study using the data from VIM. In Fig. 3, the variations with light intensity for the fitting parameters  $V_{bi}$  and  $V_{\mu}$  are presented.

The most striking result of Fig. 3 is that both  $V_{bi}$  and  $V_{\mu}$  are light-dependent for certain cells. In particular,  $V_{bi}$  decreases with light intensity for the LDLR cell, and  $V_{\mu}$  increases dramatically with light intensity for the HDHR cell, and to a lesser extent for the LDHR cell.

The changes in these parameters during LS may also reveal the internal dynamics in the cells that result in the changes in  $V_{OC}$ . The fitting parameters obtained for the cells during light-soaking are presented in Fig. 4.

The most striking element of Fig. 4 is that for both (and only) the LR cells, a visible increase in  $V_{bi}$  is observed during LS, and it is this effect that is most likely responsible for the increase in  $V_{OC}$ . Additionally, it can be noted that the LDHR cell and both the LR cells display a similar increase in  $V_{\mu}$ ,

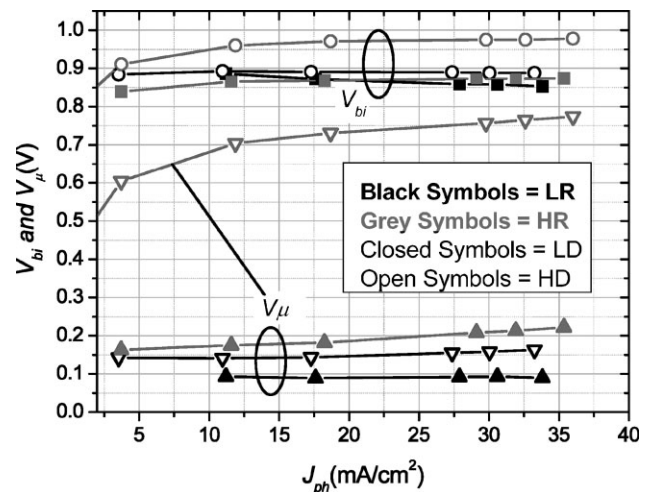


**Figure 3** Variation in fitting parameters  $V_{bi}$  and  $V_{\mu}$  with light intensity for samples in the “As Deposited” state.

although starting from different initial values. The HDHR cell shows an odd result – an improvement in  $V_{\mu}$  – but given the very light-dependent nature of both these parameters (Fig. 3), one must expect an odd internal band/defect structure for this device.

**3.4 Detailed modelling** Given the correlation between the increase in  $V_{bi}$  and one in  $V_{OC}$ , as well as the demonstrated increase in conductivity of the p-layer stacks, we use detailed numerical modelling to see if increased p-layer doping alone can account for the increased  $V_{bi}$ , and to further detail the precise physical changes resulting in this macroscopic result. We consider the results of the LDLR cell before and after light soaking.

The numerical simulations were carried out using the “AFORS-HET” (Automat FOR Simulation of HETerostructures) software, developed by the Hahn-Meitner Institut (now Helmholtz Zentrum) in Berlin [10] to

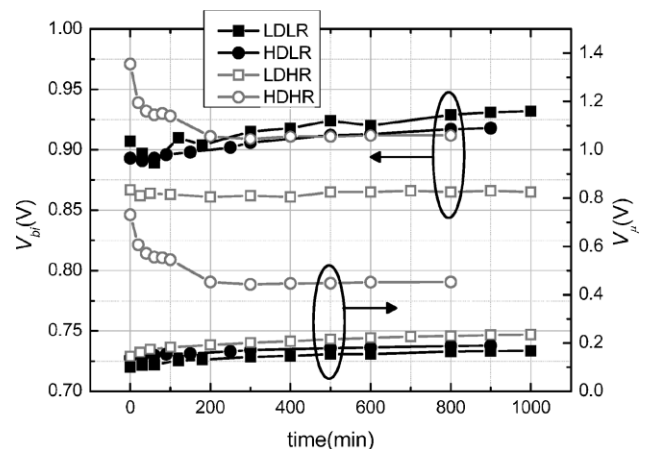


**Figure 4** Variation in fitting parameters  $V_{bi}$  and  $V_{\mu}$  with light soaking time.

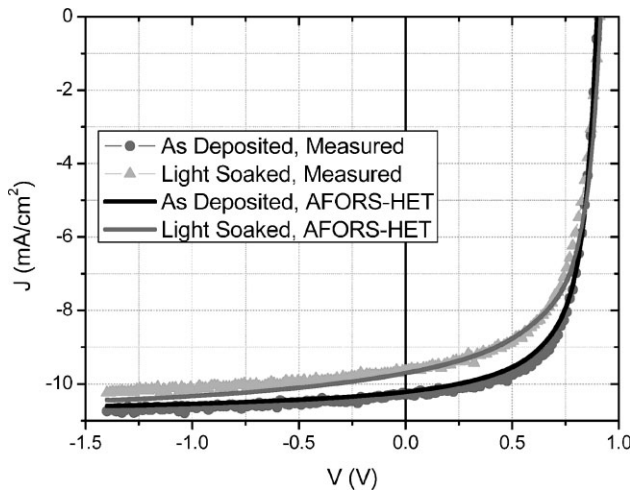


**Figure 5** Experimental  $J$ - $V$  curves at AM1.5 of LDLR cell in as deposited state (AD, dark grey symbols) and after light-soaking (LS, light grey symbols). Lines are fits obtained with AFORS-HET software.

**Table 2** Critical changes to model to fit as deposited (AD) and light soaked (LS).

	p-layer		p-i interface		i-layer	
	$E_{g,\mu}$	$N_A$	$E_{g,\mu}$	$N_{tr}$	$\mu_n$	$\mu_p$
LDLR						
AD	1.95	$1.0 \times 10^{18}$	1.95	$7 \times 10^{14}$	14	5
LS	1.98	$1.2 \times 10^{19}$	1.98	$2 \times 10^{17}$	13	3.5

study heterojunction cells. It allows the analysis of the different optical and electrical variables at any point of the solar cell, and also provides macroscopic characteristics, such as current versus voltage ( $I$ - $V$ ) and spectral response for different layer stacks, interfaces, and with different defect types and distributions in the energy bandgap of each layer. The fitting results for the LDLR cell are shown in Fig. 5 for both the as deposited and the light-soaked state. Additionally, Table 2 summarizes the critical changes necessary to the model to reproduce the  $J$ - $V$  curves.

The most interesting result of the fitting exercise is the realization that an increased doping level (even to  $1.2 \times 10^{19} \text{ cm}^{-3}$ ) is not sufficient to generate the increased  $V_{OC}$ . Rather, an increased mobility gap at the front interface is required to allow the increased  $V_{OC}$  while still reproducing the entire  $J$ - $V$  curve. This result implies that during light-

soaking, a re-distribution (in energy) of states at the interface between the p and i-layers results in this increased effective mobility gap (most importantly, on the valence band side) and allows a greater band bending across the entire device.

**4 Conclusion** Given the correlation between increases in  $V_{bi}$  and in  $V_{OC}$ , as well as the demonstrated increase in conductivity of the p-layer stack, during LS, one can clearly conclude that it is at the p-i interface that the increase in  $V_{OC}$  originates. However, the detailed device modelling suggests that it is rather the changes in the band-edge states at the p-i interface that results in the increase in  $V_{OC}$  rather than increased doping efficiency alone. A decrease in the density of valence-band edge states during LS, as these bonds break, would decrease the potential drop across this region, with limited negative consequences in terms of recombination due to the low electron density at this interface. Hydrogen accumulation in this interface region during the slower, LR growth process may accentuate the effect, and explain the lack of the effect in the HR samples.

**Acknowledgements** The portion of this work performed at the LPICM was partially supported by European Project "SE Powerfoil" (Project number 038885 SES6).

## References

- [1] E. V. Johnson, A. Abramov, Y. Soro, M. Gueunier-Farret, J. Méot, J. P. Kleider, and P. Roca i Cabarrocas, in: Proc. 23rd EU PVSEC, Valencia, Spain, 2008, 3AV.1.56.
- [2] P. St'ahel, A. Hadjadj, P. Sladek, and P. Roca i Cabarrocas, in: Proc. 14th EPVSEC, Barcelona, Spain, 1997, p. 640.
- [3] M. Isomura, H. Yamamoto, M. Kondo, and A. Matsuda, in: Proc. 2nd World PVSEC, Vienna, 1998, p. 925.
- [4] B. Rech, C. Beneking, S. Wieder, and H. Wagner, in: Proc. 14th EPVSEC, Barcelona, 1997, p. 574.
- [5] G. Yue, B. Yan, J. Yang, K. Lord, and S. Guha, in: Proc. Mater. Res. Soc. Symp. San Francisco, USA, 2003, Vol. 762, A12.2.1.
- [6] P. Roca i Cabarrocas, J. B. Chévrier, J. Huc, A. Lloret, J. Y. Parey, and J. P. M. Schmitt, J. Vac. Sci. Technol. A **9**, 2331 (1991).
- [7] J. Merten, J. M. Asensi, C. Voz, A. V. Shah, R. Platz, and J. Andreu, IEEE Trans. Electron. Devices **45**, 423 (1998).
- [8] R. S. Crandall, J. Appl. Phys. **54**, 7176 (1983).
- [9] T. Repmann, J. Kirchoff, W. Reetz, F. Birmans, J. Muller, and B. Rech, in: Proc. 3rd World Conference on Photovoltaic Energy Conversion, Osaka, Japan, 2003, p. 1843.
- [10] R. Stangl, A. Froitzheim, M. Kriegel, T. Brammer, S. Kirste, L. Elstner, H. Stiebig, M. Schmidt, and W. Fuhs, in: Proc. 19th European PVSEC, Munich, Germany, 2004, p. 1497.